

Modeling and Experimental Investigation of Reactive Shear Bands in Energetic Solids Loaded in Torsion

by

R. J. Caspar ¹, J. M. Powers ², J. J. Mason ³

Department of Aerospace and Mechanical Engineering
University of Notre Dame

presented at the

16th ICDERS
Cracow, Poland
August 1997

¹Graduate Research Assistant, present location: Gulfstream Aerospace Corporation, Savannah, Georgia

²Associate Professor

³Assistant Professor

Support

Armament Directorate of Wright Laboratories,
Eglin Air Force Base, Florida

through

Air Force Office of Scientific Research,
Research and Development Laboratories
Summer Faculty Research Program

Motivation

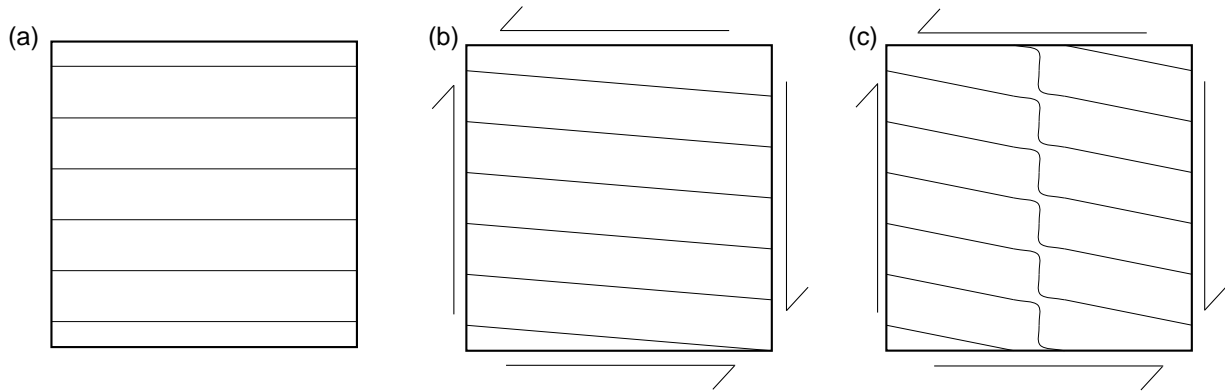
1. Development of insensitive explosives

- Risk minimization in storage and handling
- Weapon system development

2. Development of transient detonation models

- steady detonation better characterized
- late-time hydrodynamics better characterized
- early time ignition poorly understood
 - thermal stimuli
 - *mechanical stimuli, e.g. shear banding*

Shear Banding



Plastic work →

- Strain hardening
- Strain rate hardening
- Thermal softening

→ Shear localization

→ Hot spot?

→ Reaction?

Approach

1. Experiment

- Obtain data for constitutive theory (via torsional split-Hopkinson bar)
- Observe shear localization and other failure mechanisms (via ultra high speed photography)

2. Theory

- Develop model
- Implement numerical method-of-lines approach
- Predict shear localization and ignition

Novelty

1. Stress-strain-strain rate characterization of explosive simulant PBX 9501

- $C_{1.47}H_{2.86}N_{2.6}O_{2.69}$
- 95 % HMX; 2.5 % estane; 2.5 % BDNPA-F binder
- rubbery material not well suited for shear localization studies!

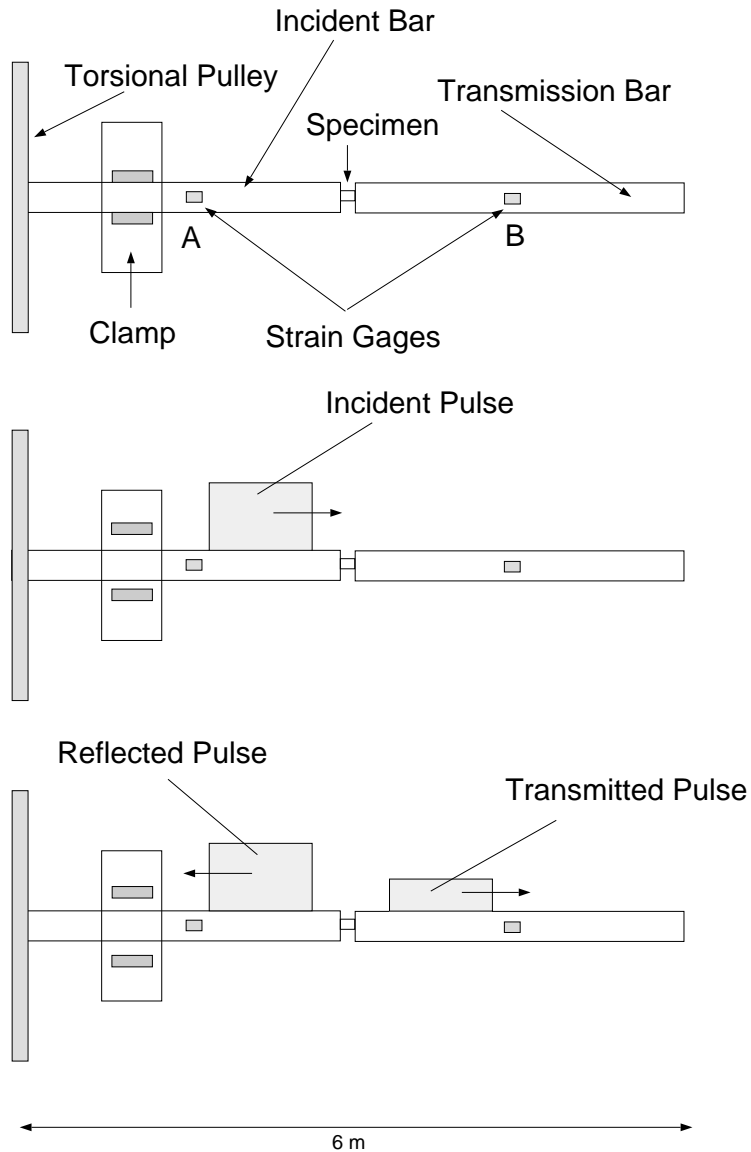
2. Extension of Frey's (1981) analysis to include strain rate effects

3. Sensitivity analysis performed

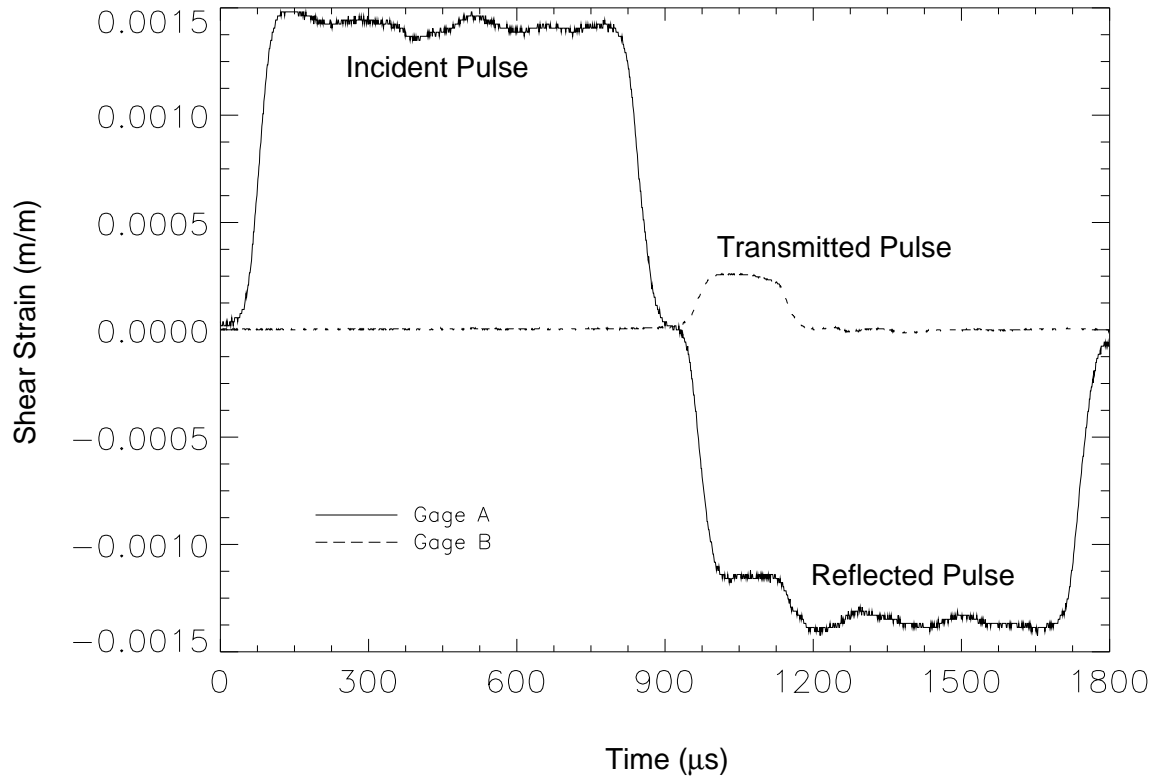
Experimental Method

Torsional Split-Hopkinson Bar

Notre Dame Solid Mechanics Laboratory



Data Analysis



Shear strain in the specimen:

$$\bar{\gamma}(t) = -\frac{2cd}{LD} \int_0^t \gamma_R(\tilde{t}) d\tilde{t}$$

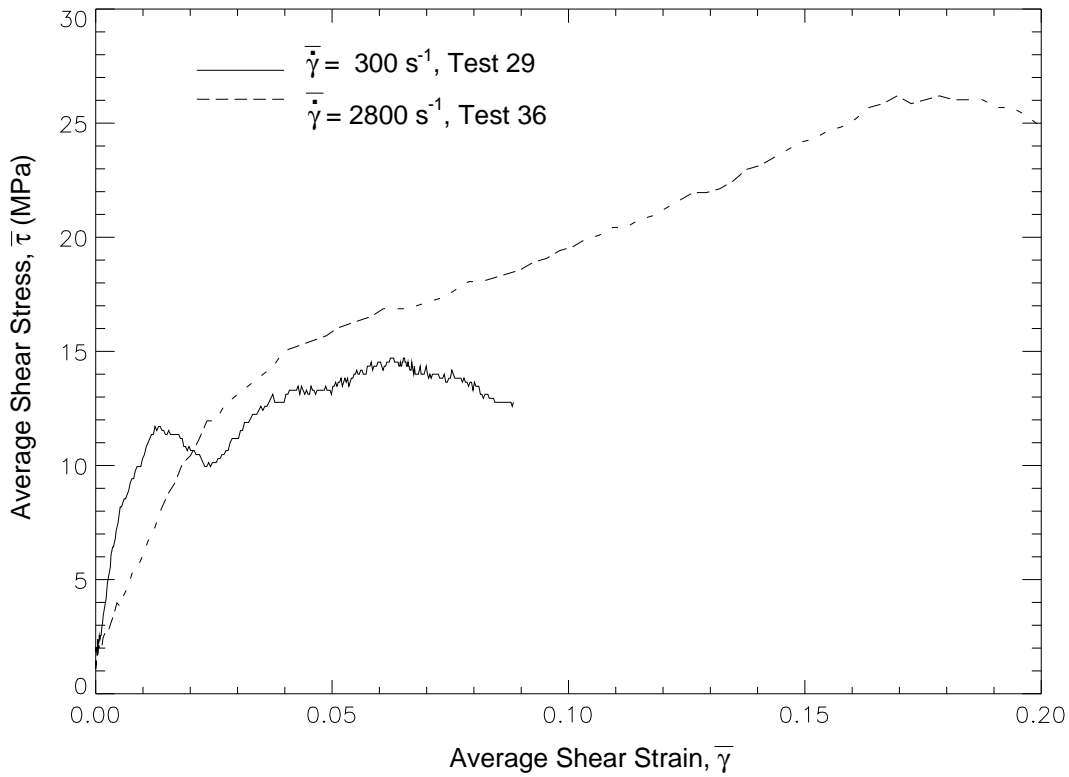
Shear stress in the specimen:

$$\bar{\tau}(t) = \frac{GD^3}{8d^2w} \gamma_T(t)$$

(Hartley, Duffy and Hawley, *Metals Handbook*, 1985)

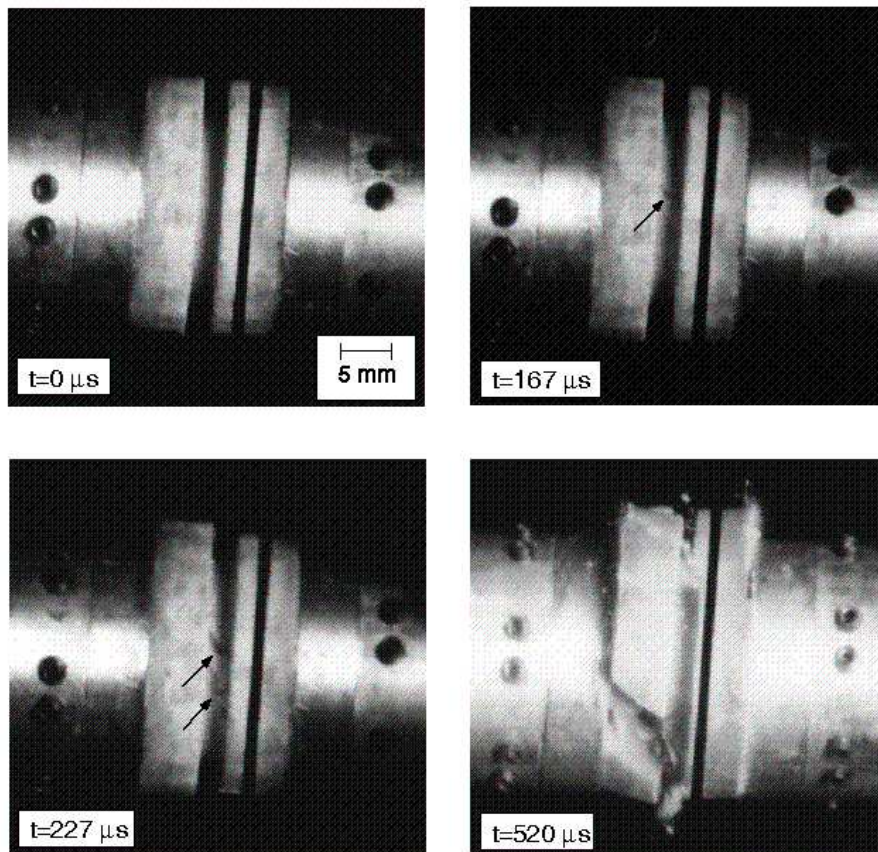
Experimental Results

Torsional Split Hopkinson Bar Tests of PBX 9501 Simulant



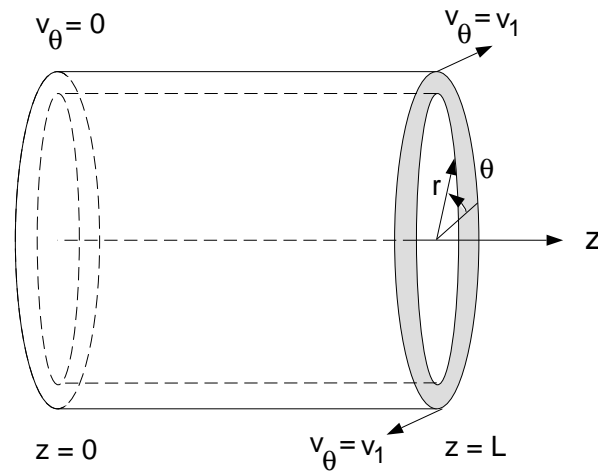
- Stress overshoot
- Lower strain rate failure \rightarrow Void nucleation and growth
- Higher strain rate failure \rightarrow Brittle fracture

Ultra-High Photography of Failure



- photos with Notre Dame's Cordon 350 camera
- failure time correlates with strain gage results

Model



- Thin walled, cylindrical specimen
- Initially unreacted, unstressed, and at ambient temperature
- $v_r = v_z = u_r = u_z = 0$
- $\frac{\partial}{\partial \theta} = \frac{\partial}{\partial r} = 0$
- Plastic work completely converted to heat
- One-step Arrhenius chemistry

Model Equations

$\rho w \frac{\partial v_\theta}{\partial t} = \frac{\partial}{\partial z} (w\tau)$	linear momentum
$\rho w \frac{\partial e}{\partial t} = w\tau \frac{\partial v_\theta}{\partial z} - \frac{\partial}{\partial z} (wq_z)$	energy conservation
$\frac{\partial \lambda}{\partial t} = Z (1 - \lambda) \exp\left(-\frac{E}{RT}\right)$	reaction kinetics
$\gamma = \frac{\partial u_\theta}{\partial z}$	strain definition
$v_\theta = \frac{\partial u_\theta}{\partial t}$	velocity definition
$\tau = \alpha T^\nu \gamma^\eta \left \frac{\partial \gamma}{\partial t} \right ^{\mu-1} \left(\frac{\partial \gamma}{\partial t} \right)$	stress relation
$q_z = -k \frac{\partial T}{\partial z}$	Fourier's Law
$e = Y_A e_A + Y_B e_B$	total internal energy
$e_A = c_A T + e_A^o$	reactant internal energy
$Y_A = 1 - \lambda$	reactant mass fraction
$e_B = c_B T + e_B^o$	product internal energy
$Y_B = \lambda$	product mass fraction
$w = w_0 - \frac{h_p}{2} \left[1 - \cos\left(\frac{2\pi z}{L_s}\right) \right]$	geometry

Reduced System

Parabolic Partial Differential Equation System

$$\frac{\partial v_\theta}{\partial t} = \frac{1}{\rho w} \frac{\partial}{\partial z} \left[w \alpha T^\nu \left(\frac{\partial u_\theta}{\partial z} \right)^\eta \left| \frac{\partial v_\theta}{\partial z} \right|^{\mu-1} \frac{\partial v_\theta}{\partial z} \right]$$

$$\begin{aligned} \frac{\partial T}{\partial t} = & \frac{1}{\rho [c_A (1 - \lambda) + c_B \lambda]} \left[\alpha T^\nu \left(\frac{\partial u_\theta}{\partial z} \right)^\eta \left| \frac{\partial v_\theta}{\partial z} \right|^{\mu+1} + \frac{k}{w} \frac{\partial}{\partial z} \left(w \frac{\partial T}{\partial z} \right) \right. \\ & \left. + Z \rho [e_A^o - e_B^o + (c_A - c_B) T] (1 - \lambda) \exp \left(-\frac{E}{RT} \right) \right] \end{aligned}$$

$$\frac{\partial u_\theta}{\partial t} = v_\theta$$

$$\frac{\partial \lambda}{\partial t} = Z (1 - \lambda) \exp \left(-\frac{E}{RT} \right)$$

Boundary Conditions

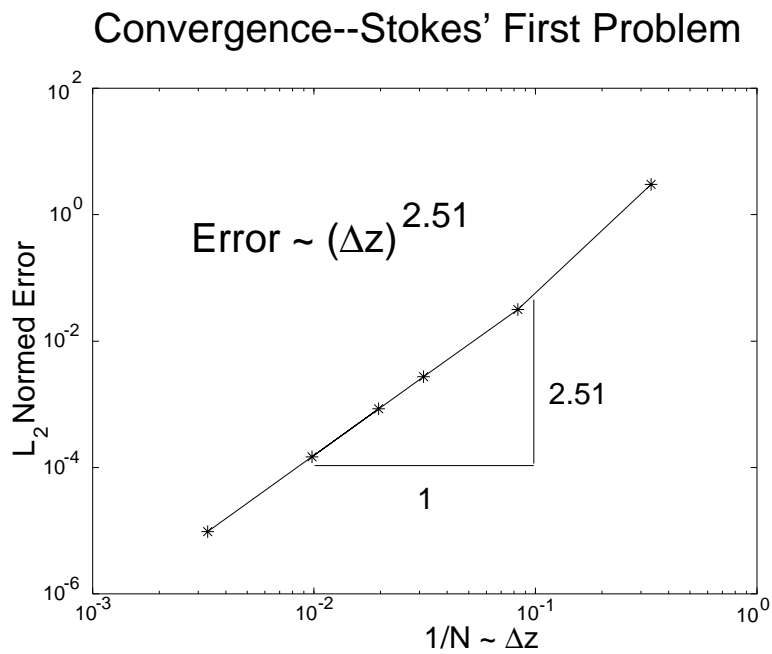
$$\begin{aligned} v_\theta(t, 0) = 0, \quad v_\theta(t, L) &= \begin{cases} (v_1 - v_0) \frac{t}{t_1} + v_0 & t < t_1 \\ v_1 & t \geq t_1 \end{cases} \\ u_\theta(t, 0) = 0, \quad u_\theta(t, L) &= \begin{cases} (v_1 - v_0) \frac{t^2}{2t_1} + v_0 t & t < t_1 \\ (v_1 - v_0) \frac{t_1}{2} + v_0 t_1 + v_1 (t - t_1) & t \geq t_1 \end{cases} \\ \frac{\partial T}{\partial z}(t, 0) = 0, \quad \frac{\partial T}{\partial z}(t, L) &= 0 \quad t \geq 0. \end{aligned}$$

Initial Conditions

$$v_\theta(0, z) = v_0 \frac{z}{L}, \quad u_\theta(0, z) = 0, \quad T(0, z) = T_0, \quad \lambda(0, z) = 0.$$

Numerical Method

- Parabolic system of PDE's—method of lines
- 2^{nd} order finite difference spatial discretization
- 4^{th} order implicit (LSODE) solution of ODE's in time



Localization Criteria

Adiabatic shear bands typically initiate at a point after a maximum stress is reached in the shear stress-shear strain relationship at that point (Zener and Hollomon, 1944):

$$\left. \frac{\partial \tau}{\partial \gamma} \right|_z \leq 0$$

With

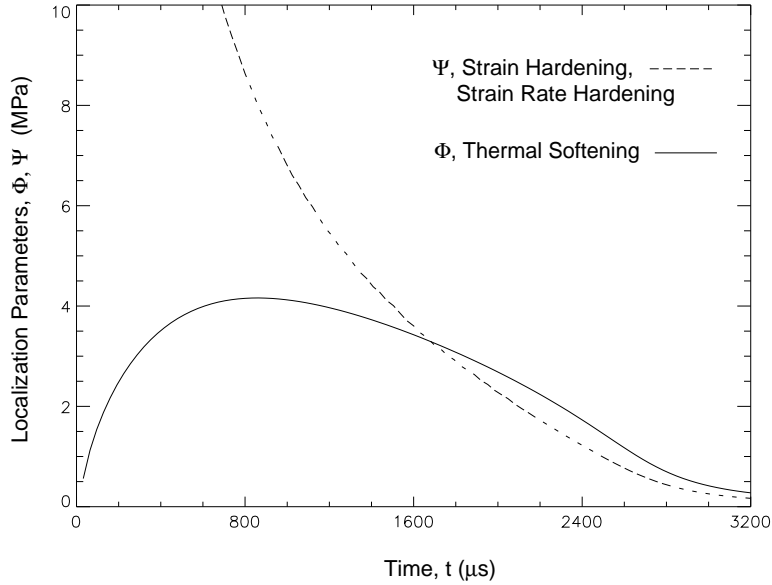
$$\tau = \tau(T, \gamma, \dot{\gamma})$$

Localization criterion (Meyers, 1994):

$$\left. \frac{\partial \tau}{\partial \gamma} \right|_{T, \dot{\gamma}} + \left. \frac{\partial \tau}{\partial \dot{\gamma}} \right|_{T, \gamma} \frac{\partial \dot{\gamma} / \partial t}{\partial \gamma / \partial t} \Big|_z \leq - \frac{\tau}{\rho c_A} \left. \frac{\partial \tau}{\partial T} \right|_{\gamma, \dot{\gamma}}$$

Theoretical Results

1. PBX 9501 without reaction, $\dot{\gamma} = 2800 \text{ s}^{-1}$

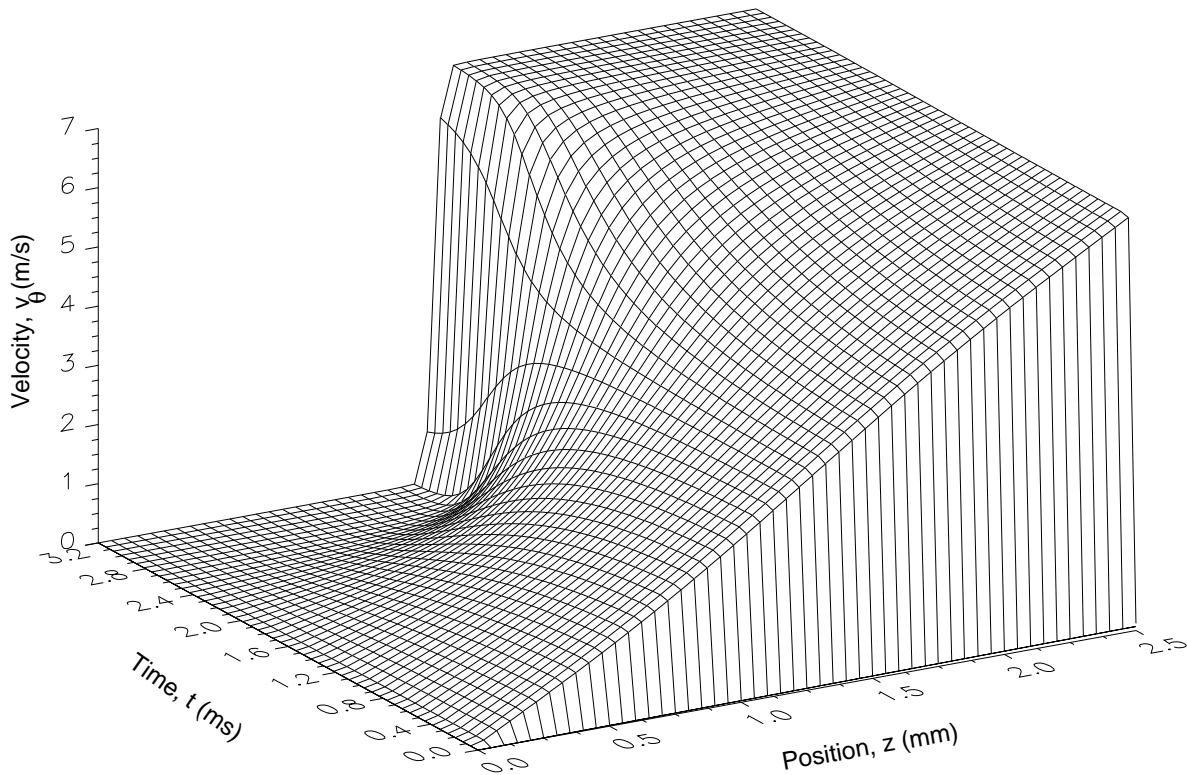


$$\left. \frac{\partial \tau}{\partial \gamma} \right|_{T, \dot{\gamma}} + \left. \frac{\partial \tau}{\partial \dot{\gamma}} \right|_{T, \gamma} \frac{\partial \dot{\gamma} / \partial t}{\partial \gamma / \partial t} \Big|_z \leq - \frac{\tau}{\rho c_A} \left. \frac{\partial \tau}{\partial T} \right|_{\gamma, \dot{\gamma}}$$

$$\Psi \leq \Phi$$

- Φ represents thermal softening
- Ψ represents strain and strain rate hardening
- Localization onset predicted after $1600 \mu\text{s}$

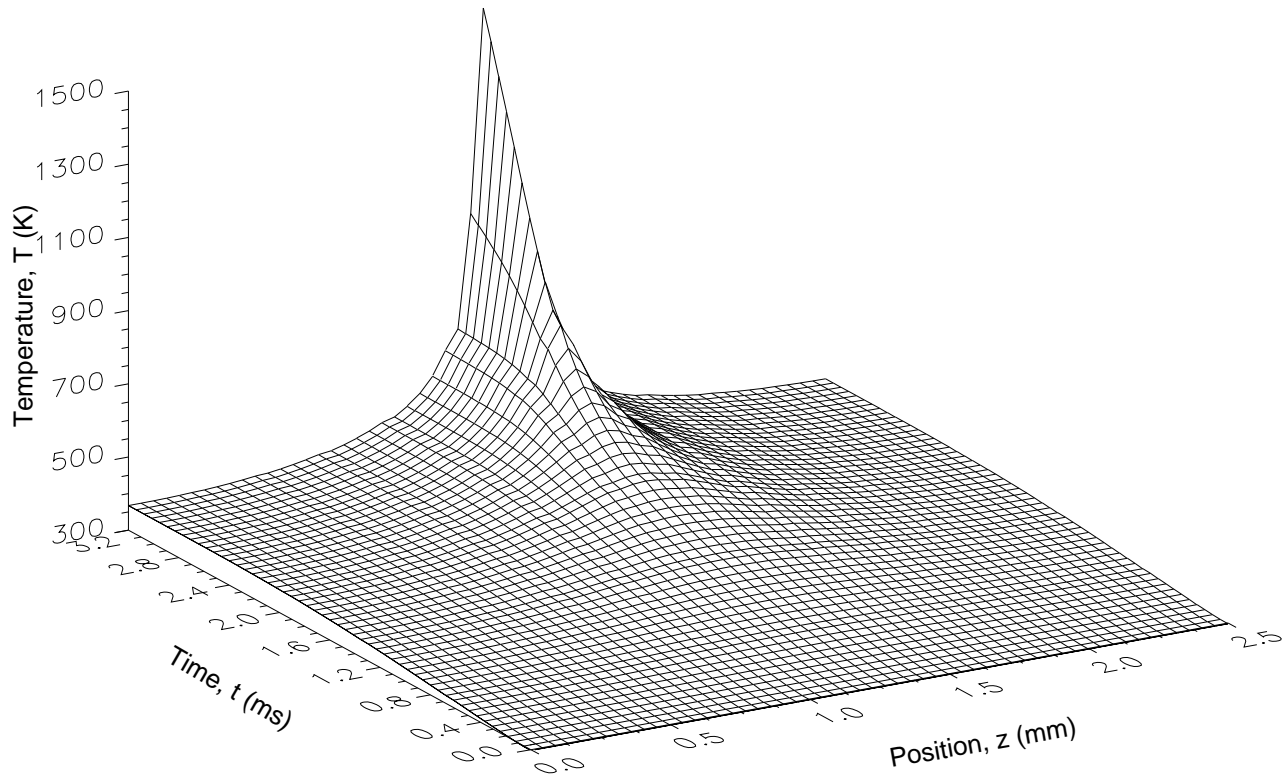
PBX 9501 without reaction, Cont.



Three stage localization process (Marchand and Duffy, 1988):

- Stage I: Homogeneous deformation
- Stage II: Inhomogeneous deformation
- Stage III: Shear band or shear localization

PBX 9501 without reaction, Cont.



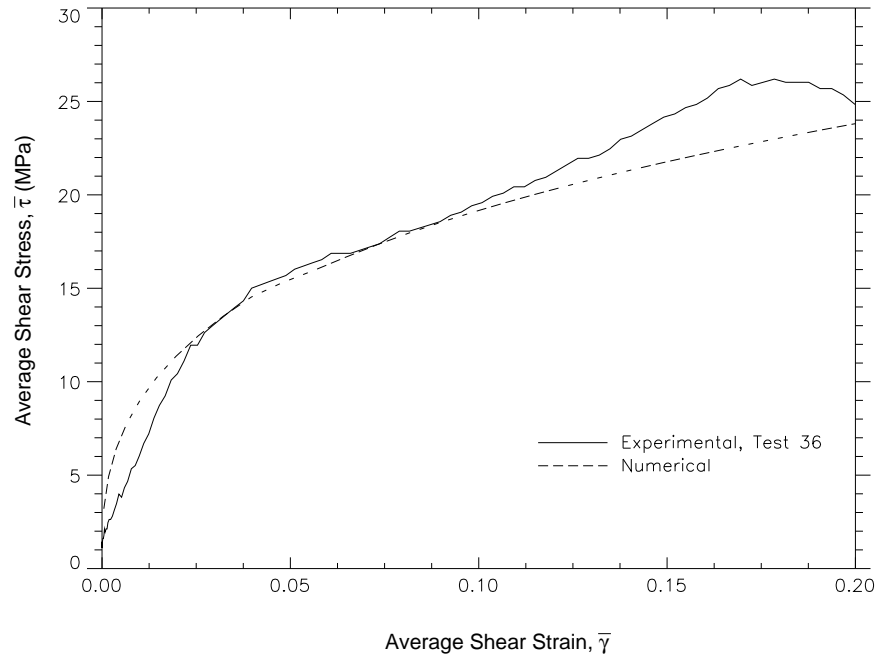
Key Issues

(a) Formation of spike following onset of localization

- After 1.67 ms , $T_{max} = 458\text{ K}$
- After 3.2 ms , $T_{max} = 1590\text{ K}$

(b) Initiation temperature is only 513 K

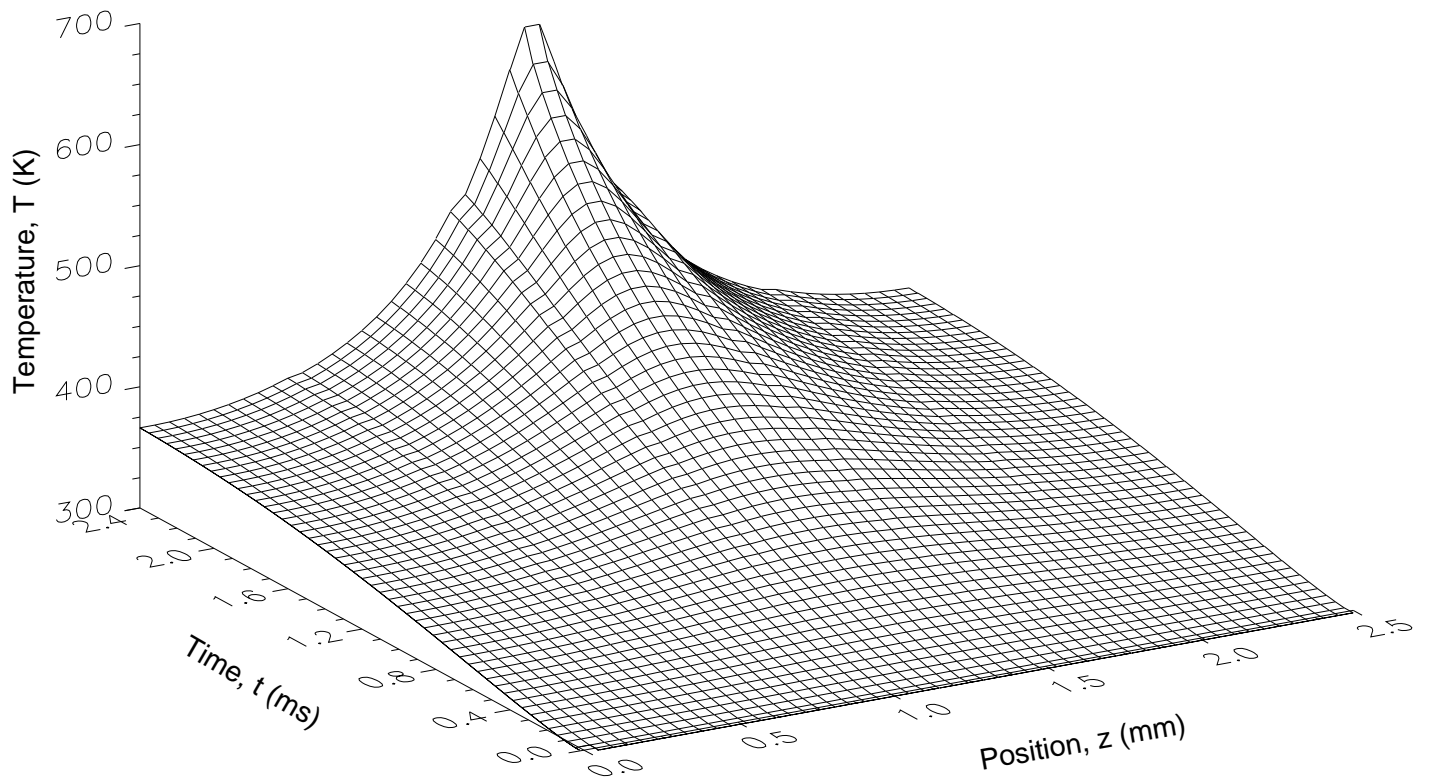
PBX 9501 without reaction, Cont.



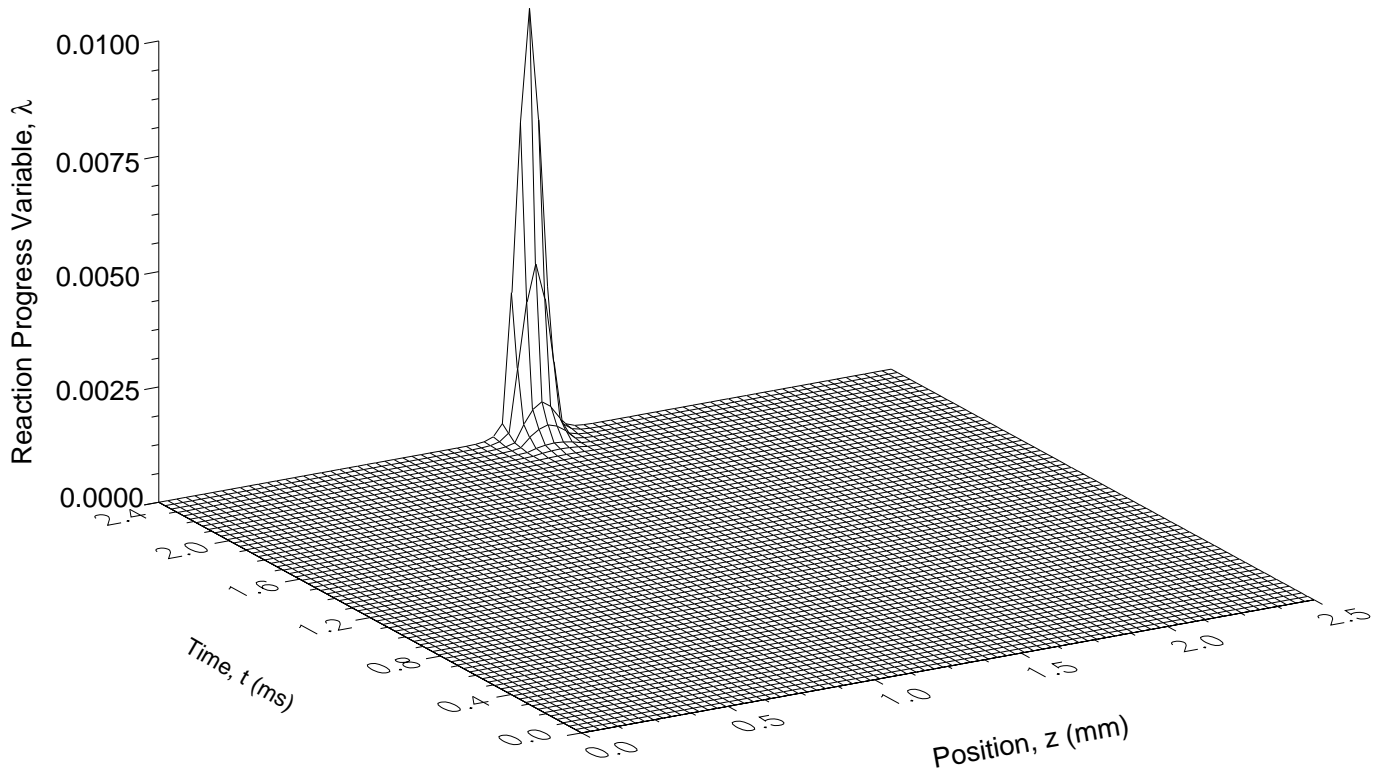
- Predictions accurate for $\bar{\gamma} \leq 0.2$
- Experimental failure at $\bar{\gamma} \approx 0.2$
- Predicted localization at $\bar{\gamma} \approx 3.5$
- Predicted failure at $\bar{\gamma} \approx 8.0$
- Failure occurs due to mechanisms other than shear localization

Theoretical Results, Cont.

2. PBX 9501 with reaction



PBX 9501 with Reaction, Cont.



- Reaction occurred before development of temperature spike
- Initiation extremely sensitive to temperature
 - No significant reaction prior to localization
 - Reaction proceeds quickly once reaction temperature reached
 - Reaction occurs at localized hot spot
- Strain at reaction is 6.4, (but experimental failure at $\bar{\gamma} = 0.2$)

Sensitivity Analysis

Parameter	Definition	Description	Value	$\hat{t}_{loc} = \frac{v_1 t_{loc}}{L}$
$\hat{\alpha}$	$\frac{\alpha T_o^\nu v_1^{\mu-2}}{\rho L^\mu}$	Stress Constant	47.019 470.19 4701.9	4.707 4.710 4.713
$\hat{\alpha} Ec$	$\frac{\alpha T_o^{\nu-1} v_1^\mu}{\rho c_A L^\mu}$	(Stress Constant)(Eckert Number)	0.0068 0.068 0.68	26.703 4.710 0.857
Pe	$\frac{\rho c_A v_1 L}{k}$	Peclet Number	8.01×10^2 8.01×10^4 8.01×10^8	4.791 4.710 4.707
\hat{Q}	$\frac{c_A^o - c_B^o}{c_A T_o}$	Scaled Heat Release	8.64 17.49 34.56	4.701 4.710 4.713
\hat{Z}	$\frac{ZL}{v_1}$	Scaled Kinetic Rate Constant	1.79×10^6 1.79×10^{11} 1.79×10^{16}	4.712 4.712 4.710
\hat{E}	$\frac{E}{RT_o}$	Scaled Activation Energy	44.52 89.04	Reaction 4.710
\hat{c}	$\frac{c_B}{c_A}$	Ratio of Specific Heats	0.5 1.0 2.0	4.715 4.710 4.705
η		Strain Hardening Parameter	0.032 0.16 0.320 0.640	1.311 4.056 4.710 Reaction
μ		Strain Rate Hardening Parameter	0.02 0.080 0.32	2.954 4.710 Reaction
ν		Thermal Softening Parameter	-0.345 -1.28	Reaction 4.710

Conclusions

- Numerical modeling indicates that if shear banding occurs, it can lead to reaction initiation
- Experiments consistently revealed failure due to mechanisms other than shear localization
 - ductile mechanisms at low strain rate, 300 s^{-1}
 - brittle mechanisms at high strain rate, 2800 s^{-1}
- Decreasing the strain and/or strain rate effects and increasing the thermal softening effect increases the susceptibility to localization

Future

- Study explosives which are more susceptible to shear banding
- Use ultra-high speed photography to observe failure ignition
- Apply hydrostatic pressure to suppress brittle failure mechanisms
- Extend models to account for material heterogeneity
- Extension to multi-dimensionality